Journal of Medicinal Chemistry

Article

A New Pyridazine Series of GABA 5 Ligands

Monique B. van Niel, Kevin Wilson, Charles H. Adkins, John R. Atack, Jos L. Castro, Dawn E. Clarke, Stephen Fletcher, Ute Gerhard, Mark M. Mackey, Sallie Malpas, Karen Maubach, Robert Newman, Desmond O'Connor, Gopalan V. Pillai, Peter B. Simpson, Steven R. Thomas, and Angus M. MacLeod

J. Med. Chem., **2005**, 48 (19), 6004-6011• DOI: 10.1021/jm050249x • Publication Date (Web): 23 August 2005

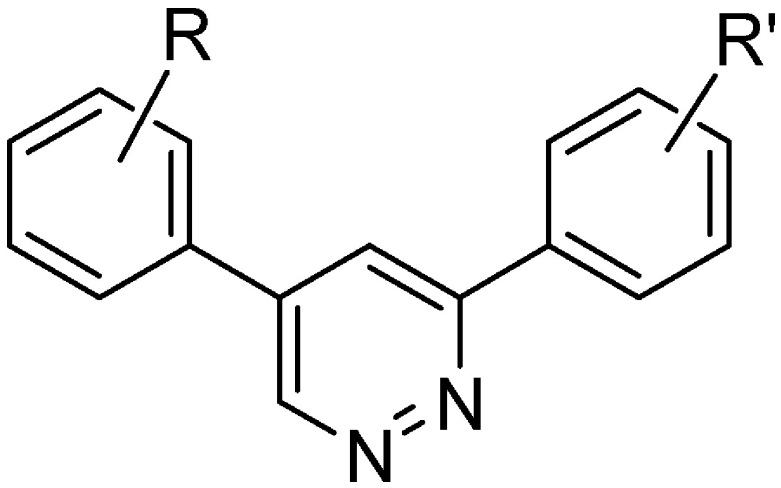

More About This Article

Additional resources and features associated with this article are available within the HTML version:

- Supporting Information
- Access to high resolution figures
- Links to articles and content related to this article
- Copyright permission to reproduce figures and/or text from this article

View the Full Text HTML

Journal of Medicinal Chemistry is published by the American Chemical Society. 1155 Sixteenth Street N.W., Washington, DC 20036

A New Pyridazine Series of $GABA_A$ α5 Ligands

Monique B. van Niel,* Kevin Wilson,* Charles H. Adkins, John R. Atack, José L. Castro, Dawn E. Clarke, Stephen Fletcher, Ute Gerhard, Mark M. Mackey, Sallie Malpas, Karen Maubach, Robert Newman, Desmond O'Connor, Gopalan V. Pillai, Peter B. Simpson, Steven R. Thomas, and Angus M. MacLeod

Departments of Medicinal Chemistry, Biochemistry and Pharmacology, Merck Sharp & Dohme Research Laboratories, Terlings Park, Eastwick Road, Harlow, Essex, CM20 2QR, United Kingdom

Received March 18, 2005

Screening of the Merck compound collection identified **6** as an unusually simple, low molecular weight hit with moderate affinity for $GABA_A$ receptors. The structural novelty of **6**, compared to our advanced series of $GABA_A$ α5 inverse agonists, made it an attractive molecule for further exploration. This paper will describe the evolution of **6** into a new series of ligands with nanomolar affinity and functional selectivity for $GABA_A$ α5 receptor subtypes.

Introduction

$GABA_A$ ligand-gated ion channels play a key role during fast inhibitory neurotransmission in the mammalian central nervous system and are activated by the endogenous neurotransmitter γ-aminobutyric acid (GABA). Additional binding sites have been found on the $GABA_A$ ion channel at which synthetic compounds, including anaesthetics, avermectins, barbiturates, benzodiazepines and loreclezole exert their predominant pharmacological actions. Some of these binding sites influence the binding of GABA, and this allosteric, pharmacological modulation, results in changes in flux of chloride through the ion channel, with concomitant effects on neuronal activity and disease states.

Of particular interest is the site that binds benzodiazepines, for which no endogenous ligand has so far been identified. At this site, exogenous ligands can be classed as positive allosteric modulators (full agonists, e.g. diazepam) which enhance the effects of GABA and increase the chloride flux: negative allosteric modulators (inverse agonists, e.g. 6,7-dimethoxy-4-ethyl-β-carboline-3-methoxylate, DMCM) which decrease chloride flux: or antagonists (e.g. flumazenil) which cause no overall change in chloride flux but can prevent agonists or inverse agonists from binding.

Full agonists such as diazepam have been in clinical use as anxiolytics, anticonvulsants and sedatives since the 1960s. Memory impairment and dependence are associated adverse side effects. Inverse agonists produce converse behaviors including anxiety and convulsions, and they can augment the activity of convulsant compounds when they are coadministered (proconvulsant profiles). For these reasons, inverse agonists have, to date, only been used as research tools. Of particular interest is the observation that inverse agonists enhance learning and memory in animals and this indication has been actively studied in several laboratories.[1]

Molecular biology studies in the late 1980s and early 1990s demonstrated that the $GABA_A$ channels are formed from pentameric assemblies of 16 different subunits (α1−α6, β1-β3, γ1−γ3, δ, ϵ, θ, π).[2,3] Evolution has favored a small number of combinations and the more abundant assemblies α1β2γ2, α2β3γ2, α3β3γ2, and α5β3γ2 show distinct regional distribution in the brain. Ion channels containing an α5 subunit account for 25% of GABA receptors in the hippocampus, an area of the brain implicated in learning and memory.[4] Disease states such as dementias do not affect the population density of α5-containing receptors in the hippocampus, making them an attractive target for therapeutic intervention. Additional evidence for the role of this subtype in hippocampal function has come from transgenic mouse models in which α5 subunits are absent or decreased in the hippocampus. These animals showed enhanced performance in learning and memory tests[5,6] giving support to the hypothesis that α5 inverse agonists would be cognition enhancers.

After three decades of benzodiazepine use, it was established through use of recombinant receptors that binding of these drugs occurs exclusively at the interface of the α and γ subunits.[7−10] The commonality of the binding contribution made by the γ2 subunit this makes the discovery of binding selective compounds a significant challenge. Unpleasant side effects, such as sedation seen with benzodiazepine agonists or seizures observed with inverse agonists such as DMCM, are a consequence of the nonselective nature of these compounds and targeting drugs with single receptor subtype selectivity may result in drugs with improved profiles. The transgenic mice described above do not show an increase in seizure activity, suggesting that selective α5 inverse agonists would be cognition enhancers devoid of unwanted side effects. Following on from elegant biology came the challenge to medicinal chemists to identify subtype selective molecules[11] which would enable clinical evaluation of the hypothesis.

With these aims in mind, we have recently reported the identification of **1**,[12] **2**,[13] **3**[14] and **4**[15] as α5 $GABA_A$ inverse agonists which are cognition enhancing in rodent models (Chart 1). As part of a back-up strategy, a search for truly structurally diverse leads to complement existing series was initiated by screening of compounds in the Merck collection for affinity at α1, α3 and α5 $GABA_A$ receptor subtypes. Methyl 1,5-diphenyl-

* To whom correspondence should be addressed. Tel +44 (0)1279 440000; Fax +44 (0) 1279 440390; e-mail: monique_vanniel@merck.com and kevin_wilson2@merck.com.

10.1021/jm050249x CCC: $30.25
Published on Web 08/23/2005

Chart 1

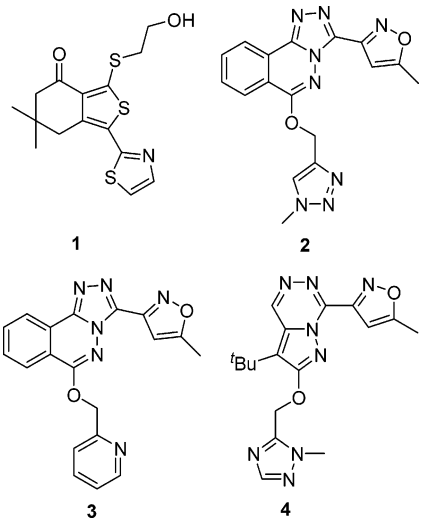

2,3-diazabicyclo[3.1.0]hex-2-ene-6-carboxylate (**5**)[16,17] was identified as an interesting lead with good affinity for GABA$_A$ α5 receptors (Chart 2). Subsequent assessment

Chart 2

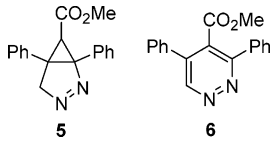

of the original stored solution revealed that the sample had rearranged and oxidized to form the pyridazine **6**.[18] Rescreening of a sample prepared by independent synthesis confirmed that **6** was responsible for the observed binding affinity. The low molecular weight and intriguingly simple structure of **6** made it an attractive molecule for further exploration.[19] This paper will describe the evolution of **6** into a new series of ligands with nanomolar affinity and functional selectivity for GABA$_A$ α5 receptor subtypes.

Synthetic Chemistry

(a) 3-Phenyl-5-arylpyridazines. Chemistry was initiated with a resynthesis of screening lead **6**.[18] Having confirmed that **6** was responsible for the observed binding affinity at GABA receptors, further work was instigated to explore preliminary structure−activity relationships (SAR) of this lead. To determine the importance of the ester for binding affinity, pyridazine **7** was prepared using stannane **8**[20] (Scheme 1). The finding that **7** retained good binding affinity and was accessible via an advanced intermediate made this molecule a more attractive lead for further evaluation.[21,22] The low molecular weight of pyridazine **7** would also accommodate a number of options for optimizing in vitro and in vivo profiles by increasing the complexity of the molecular architecture. It was also anticipated that the stannane **8** could be reacted in parallel using solution phase synthesis in a microwave reactor.[23] Multiple Stille couplings could be performed in a short time frame using simple apparatus. The stannane **8** was also converted to the iodide **9**[20] (Scheme 1) which allowed incorporation of a complementary set of aryl boronic acids using a microwave reactor as described

Scheme 1[a]

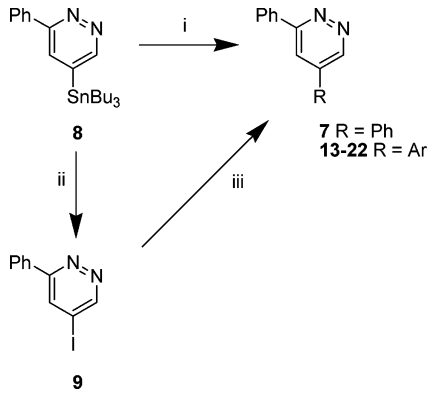

[a] Reagents: (i) Pd(PPh$_3$)$_4$, THF, ArBr, 150 °C, 600 s, microwave reactor; (ii) I$_2$, THF; (iii) Pd(PPh$_3$)$_4$, THF, 2N Na$_2$CO$_3$, ArB(OH)$_2$, 150 °C, 600 s, microwave reactor.

above. Our in-house diversity program[24] was used to select a set of 50 aryl boronic acids and halides to fully capture a diverse selection of reagents to explore chemical space at the 5-position of the pyridazine. A smaller set of 10 proprietary and privileged fragments to add further diversity coverage and novelty was also selected. Following simple workup, products were purified by HPLC with mass triggered fraction collection or crystallization. The overall process was very efficient, with the design and synthesis of several small targeted libraries, through iterative loops, being achieved in a short time frame.

(b) 3,5-Diarylpyridazines. Following identification of a number of interesting leads from this initial work (see below), our attention also focused on modifications to the 3-aryl substituent. Accordingly, 5-chloropyridazin-3(2*H*)-one **10**[25] was identified as a valuable intermediate that enabled the incorporation of 5-aryl substituents using a Suzuki coupling (Scheme 2). Only minor modi-

Scheme 2[a]

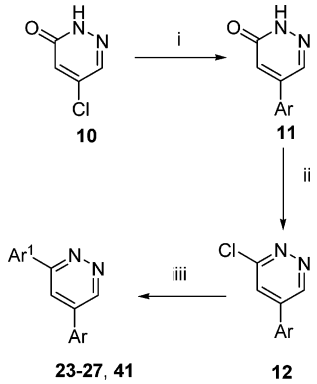

[a] Reagents: (i) dichloro-(1,4-bis(diphenylphosphino)butane), PhCH$_3$, Na$_2$CO$_3$, ArB(OH)$_2$, 150 °C, 600 s, microwave reactor; (ii) POCl$_3$; (iii) dichloro-(1,4-bis(diphenylphosphino)butane)palladium, THF, Na$_2$CO$_3$, Ar^{1}B(OH)$_2$, 150 °C, 600 s, microwave reactor.

fications to the catalyst and solvent used in the original protocol were required. Conversion of the 5-arylpyridazinones **11** to the chloride **12** enabled further functionalization to be carried out at the 3-position using an additional Suzuki coupling. This sequence gave efficient access to a range of 3,5-diaryl substituted pyridazines for evaluation.

(c) 3-Amino- and 3-Alkoxy-5-arylpyridazines. 5-Aryl-3-chloropyridazines **12** were also ideal substrates

Scheme 3[a]

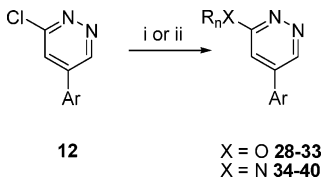

[a] Reagents: (i) ROH, Na; (ii) R_2NH, THF, 170 °C, microwave reactor, 600 s.

to explore amine and alkoxide substitution at the 3-position. Displacement of the chloride occurred rapidly with freshly generated alkoxides at room temperature or with amines under microwave conditions (Scheme 3).

Results and Discussion

Binding Affinity. Although removal of the ester of **6** to form **7** did not give an enhanced in vitro binding profile, it did clearly simplify the pyridazine core structure and improved synthetic access. Both pyridazine nitrogen atoms are absolutely required to achieve good binding affinity, and their role is subtle. Thus 2,4- and 3,5-diphenylpyridine and 4,6-diphenylpyrimidine have no affinity for any receptor subtypes (K_i > 600 nM). 3,5-Diphenyl-1,2,4-triazine and 4,6-diphenyl-1,2,3-triazine were the only alternative heterocycles that retained weak affinity (α5: K_i = 160 nM and 300 nM, respectively), and our SAR was thus confined to the original 3,5-diphenylpyridazine (**7**). Preliminary efforts were focused on modifications to the 5-phenyl group. From our first parallel synthesis run it became apparent that *meta*-substitution of this phenyl ring was favored over the ortho or para positions. For example, the *m*-cyano substituent **15** had nanomolar binding affinity at α5 receptors whereas **13** and **14** were at least 10 fold weaker (Table 1). Additional substituents that followed this observation include bromo (**16**), isopropoxy (**17**) and methyl carboxylate (**18**) groups. Thiophene **19** was also identified in the first library and had a similar binding profile when compared to the phenyl isostere **18**. The strategy to use a diverse set of aryl halides reagents during the first targeted library was clearly valuable in identifying further interesting lead compounds with improved binding affinities at α5 receptors. Another beneficial strategy was to include proprietary fragments. Compounds **20** and **21**, substituted with heterocycles, also showed improved in vitro profiles, with **22** having the highest observed affinity at all receptor subtypes.

On the basis of binding affinity and efficacy profiles (see below), **15** was selected for further elaboration. Fluorine plays a pivotal role in the life sciences industry as a result of its ability to modify molecular properties including lipophilicity, metabolic stability and conformation in addition to binding affinities. This substituent was therefore incorporated on the 3-phenyl ring. We observed that only 2-fluoro (**23**) and 3-fluoro (**24**) substitution retained low nanomolar binding affinity for the α5 receptor subtype. Derivatives **25**−**27** had weaker binding affinity, and this gave us preliminary indications about substitution patterns which may be tolerated.

Replacement of the 3-phenyl group with alkoxides and amines was also pursued. Brief exploration with alkoxide substituents showed that ethoxide (**29**) did retain respectable binding affinity. However, whereas **15** and **16** had been equipotent in the biaryl pyridazine series, **33** was 7-fold less active at α5 than the corresponding bromide **29**. Introduction of some simple alkyl amino substituents such as **36**, **37** and **40** were also tolerated. Interestingly, the affinity for **36** and **38** tracked that observed with the corresponding alkoxide pairs **29** and **33** , but in contrast to this, **40** had higher affinity than **39**. Thus, amine and alkoxide substitution could offer useful alternative scaffolds with additional structural variation, for further optimization.

A comparison of **41** with **15** illustrates that substituents are not transferable from the 5-position to the 3-position of the pyridazine. This observation supported our earlier conclusions regarding the subtle directional influences of the nitrogen atoms.

Functional Efficacy. The pyridazines, in common with our previously reported structural classes,[12−15] have modest binding selectivities for the receptor subtypes. With binding selectivities of less than an order of magnitude, discrimination between the receptor subtypes was targeted through functional selectivity. Patch-clamp electrophysiological techniques were used to determine functional efficacy. Although this generates high quality data, it has low capacity for screening purposes, and the multiple compounds generated from parallel synthesis could not be evaluated efficiently in this manner. Primary functional screening data was thus generated using a voltage/ion probe reader (VIPR)[26,27] assay as an aid in the selection of compounds which would be more fully evaluated.

We were encouraged to note that while **7** retained a respectable in vitro binding profile it was also a weak inverse agonist at α5 receptors in the VIPR functional assay. It became apparent from the early analogues which were prepared in this pyridazine series that α5 functional selectivity could be modulated through incorporation of simple substituents in the C5 phenyl ring. In addition to improving binding affinity, the *m*-cyano (**15**), methyl carboxylate (**18**) and triazole analogue (**20**) were also functionally selective inverse agonists for α5 receptor subtypes. The nature of the substituent clearly plays a crucial role in influencing efficacy profiles, with analogues **16**, **17**, **19**, **21** and **22** demonstrating a range of efficacies at α5 receptors and functional selectivities over other receptor subtypes.

Assessment of fluorinated analogues **23**−**27** in the VIPR assay indicated that only **23** retained a balance of binding affinity and α5 functional selectivity. There were indications that heteroatom-linked pyridazines such as **29**, **36**, **37** and **40** could attain good affinity at α5 receptors although only **36** showed α5 functional selectivity.

Clearly, the primary binding and functional assays acted as efficient, but stringent, filters for the compounds generated using parallel synthesis. We were encouraged to identify **15**, **23** and **36** since they had desired in vitro profiles. Analogue **15** was selected for full evaluation of efficacy profiles. Measurements in mouse fibroblast L(tk$^-$) cells expressing human $GABA_A$ receptor subtypes demonstrated that **15** was an α5 inverse agonist (efficacy = −37%) as predicted using VIPR (Table 2). Reference compounds include non selective DMCM which is regarded as a α5 full inverse

Table 1. Binding Affinity and Efficacy of Pyridazines at Human Recombinant GABA$_A$ αxβ3γ2 Receptor Subtypes

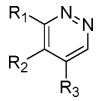

				binding affinity K_i, nM[a]			efficacy[b]	
	R^1	R^2	R^3	α1	α3	α5	α3	α5
6	Ph	CO_2CH_3	Ph	154 ± 48	64 ± 25	12 ± 3	n.d	27 ± 6
7	Ph	H	Ph	36 ± 4	45 ± 6	29 ± 6	−20 ± 11	−14 ± 10
13	Ph	H	2-CN-Ph	n.d	440 ± 41	323 ± 33	n.d.	n.d.
14	Ph	H	4-CN-Ph	27 ± 3	81 ± 9	56 ± 7	49 ± 11	45 ± 9
15	Ph	H	3-CN-Ph	7.0 ± 3.7	14 ± 4	5.2 ± 1.3	−4 ± 7	−32 ± 6
16	Ph	H	3-Br-Ph	7.5 ± 1.9	15 ± 3	7.9 ± 2.2	−2 ± 9	−2 ± 9
17	Ph	H	3-O^{i}Pr-Ph	12 ± 4	27 ± 8	8.4 ± 2.5	22 ± 10	18 ± 9
18	Ph	H	3-CO_2CH_3-Ph	n.d	29 ± 10	11 ± 1	−7 ± 6	−48 ± 7
19	Ph	H		88 ± 17	45 ± 8	12 ± 3	−44 ± 6	−39 ± 5
20	Ph	H		n.d	41 ± 3	12 ± 2	13 ± 11	−31 ± 6
21	Ph	H	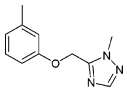	8.5 ± 1.1	10.4 ± 1.0	8.8 ± 1.4	43 ± 14	−5 ±16
22	Ph	H		1.3 ± 0.1	3.1 ± 0.1	1.6 ± 0.2	−49 ± 4	−62 ± 14
23	2-F-Ph	H	3-CN-Ph	n.d.	7.9 ± 0.9	3.4 ± 0.3	−17 ± 10	−31 ± 14
24	3-F-Ph	H	3-CN-Ph	n.d.	7.2 ± 1.6	4.0 ± 0.4	3.6 ± 9	0 ± 10
25	4-F-Ph	H	3-CN-Ph	n.d.	26 ± 12	14 ± 3	n.d.	n.d.
26	2,4-diF-Ph	H	3-CN-Ph	n.d.	23 ± 1	17 ± 7	n.d.	−57 ± 7
27	3,4-diF-Ph	H	3-CN-Ph	n.d.	41 ± 9	13 ± 4	32 ± 15	−15 ± 12
28	OMe	H	3-Br-Ph	n.d.	205 ± 81	54 ± 18	42 ± 14	−18 ± 14
29	OEt	H	3-Br-Ph	8.6 ± 1.2	19 ± 1	5.7 ± 3.1	39 ± 5	4 ± 7
30	O^{i}Pr	H	3-Br-Ph	26 ± 1	60 ± 9	36 ± 4	28 ± 9	12 ± 12
31	OBn	H	3-Br-Ph	n.d.	302 ± 100	63 ± 23	32 ± 13	n.d.
32	OBn	H	3-CN-Ph	n.d.	60 ± 8	17 ± 2	60 ± 10	n.d.
33	OEt	H	3-CN-Ph	n.d.	72 ± 9	36 ± 4	19 ± 10	−9 ± 6
34	NHMe	H	3-Br-Ph	49 ± 19	113 ± 12	27 ± 11	3 ± 6	−26 ± 5
35	NMe_2	H	3-Br-Ph	55 ± 6	120 ± 13	51 ± 1	−49 ± 4	−62 ± 14
36	NHEt	H	3-Br-Ph	3.5 ± 1.2	7.3 ± 1.6	3.8 ± 1.1	2 ± 8	−12 ± 7
37	NH^{i}Pr	H	3-Br-Ph	7.3 ± 0.2	22 ± 9	7.2 ± 2.0	25 ± 10	14 ± 9
38	NHEt	H	3-CN-Ph	n.d.	79 ± 6	33 ± 5	8 ± 13	−29 ± 10
39	NHBn	H	3-Br-Ph	n.d.	51 ± 5	19 ± 7	66 ± 10	14 ± 7
40	NHBn	H	3-CN-Ph	n.d	15 ± 5	6.1 ± 0.1	59 ± 11	17 ± 16
41	3-CN-Ph	H	Ph	>666	>666	>666	n.d.	n.d.

[a] Displacement of [^{3}H] Ro 15-1788 binding from human recombinant GABA$_A$ αxβ3γ2 receptor subtypes (x = 1, 3 or 5) stably expressed in mouse fibroblast L(tk$^-$) cells. K_i values are the mean ± SEM of at least three independent determinations. [b] Primary functional screening datawere generated using a Voltage/Ion Plate reader assay[26,27] at compound concentrations of 300 nM. n.d., not determined.

Table 2. Maximum Inhibition and pEC$_{50}$ Values of a GABA EC$_{20}$ Response Produced by **15** at Human GABA$_A$ Receptor Subtypes Expressed in L(tk$^-$) Cells

subunit	α1	α3	α5
maximum inhibition (%)[a]	−23 ± 2[b]	−16 ± 2[c]	−37 ± 5[b]
pEC$_{50}$[d]	−8.53 ± 0.27	−8.02 ± 0.47	−8.13 ± 0.03

[a] Values are the mean maximum modulation ± SEM from [b]n = 4; [c]n = 3 concentration−response curves for each receptor subtype. [d] Negative logarithm of the concentration that leads to 50% maximal response.

agonist (efficacy = −52%),[13] the full agonist chlordiazepoxide (efficacy = +134%)[13] and in house clinical candidates **2**[13] (efficacy = −40%) and **4**[15] (efficacy = −55%). **15** was found to have a weak partial inverse agonist profile at α1 and α3 subtypes. An ideal profile at these receptor subtypes would be an antagonist profile in order to prevent undesirable biological activity resulting from activation of these receptors. However, there was a window of functional selectivity, and this provided the opportunity to evaluate this compound further in our screening cascade.

Pharmacokinetics. The pyridazine **15** was evaluated for pharmacokinetic (PK) properties in rat. A low volume of distribution together with clearance of approximately half-liver blood flow resulted in a half-life of 0.6 h. Exposure of pyridazine **15** to isolated rat liver microsomes showed that 46% of the material was metabolized in 15 min (Table 3). These data was useful to correlate with the observed pharmacokinetics. Additionally, microsomal turnover in higher species demonstrated that **15** was extensively metabolized in dog, rhesus and human liver microsomes. If turnover data is assumed to be a good predictor for pharmacokinetics in rat, then it may be extrapolated that PK parameters are likely to be poor in the higher species. Our attempts to address potential metabolism issues, by incorporation

Table 3. Pharmacokinetics and Microsomal Turnover for **15**

	NADPH dependent turnover in liver microsomes (%)[a]				pharmacokinetics[b]		
	rat	dog	rhesus	human	Cl[c]	$T_{1/2}$[d]	V_{dss}[e]
15	46 ± 8	86 ± 1	89 ± 1	85 ± 0	36	0.6	1.5

[a] $n = 3$, mean ± SD. [b] 1 mg/kg in a single rat of a 3:1 PEG 300: water solution given iv (1 mL/kg). [c] mL/min/kg from plasma. [d] Hours, calculated from 1 to 3 h data. [e] L/kg.

of fluorine substituents, provided limited access to analogues with both the desired in vitro binding and functional efficacy profiles. Our conclusions from progressing **15** down the screening cascade were that there are number of challenges which need to be addressed in developing the SAR of this lead.

Conclusions

We have described how screening hit **6** was identified as a pyridazine with moderate affinity for the α5 receptor subtype of the $GABA_A$ ligand-gated ion channel. Initial SAR resulted in the identification of the low molecular weight, structurally simple 3,5-diphenylpyridazine (**7**) which retained respectable binding affinity and was an inverse agonist at α5 receptors. This lead was explored using parallel synthesis which resulted in the identification of compounds such as **15** and **23** with improved binding affinity which were more efficacious inverse agonists at α5 receptors. The identification of functionally selective leads such as **15** may be useful in further delineating the complex biology of the GABA-A receptor complex in vivo. Our observations that simple, low molecular weight structures could provide functionally selective ligands were unexpected when we started to evaluate the original screening hit. The results reported above encouraged us to carry out additional extensive studies, the results of which will be described in a following paper.

Experimental Section

Radioligand Binding Assay at the Benzodiazepine Site. The binding affinities of synthesized molecules for various subtypes of $GABA_A$ receptors were determined by automated radioligand binding.[10] Membrane pellets, prepared from Ltk$^-$ cells expressing $GABA_A$ receptors of subunit composition $\alpha1\beta3\gamma2$, $\alpha3\beta3\gamma2$ or $\alpha5\beta3\gamma2$, were resuspended in different volumes of ice-cold 50 mM Tris assay buffer, depending on the total cpm they gave when batch tested, using a Polytron for 10 s. Test compounds were prediluted from 2 mM stocks to 100 μM in DMSO followed by a final dilution into buffer, and the incubation was started with the addition of membranes. Inhibition of specific [^{3}H]Ro15-1788 binding (specific activity 78.6Ci/mmol, NEN) was measured for 30 min at 24 °C in 50 mM Tris buffer, pH 7.4. The final concentration of radioligand was 1.8 nM. Nonspecific binding was defined with 10 μM flunitrazepam (Sigma, UK), and total binding was determined in the presence of 0.1% DMSO. The assays were performed using a Sagian Robotic system. The assay was terminated by filtration over prewetted Unifilter GFB plates (Packard, UK) using an automated Brandel harvestor, washing with Tris buffer. Filter plates were dried for 4−6 h at room temperature, and the robot then added 50 mL of Microscint 'O' to each well of the filter plate, incubating for 1 h. Following this, plates were counted for 1 min/well in a TriLux to detect filter-retained radioactivity. Results were generated using ActivityBase and the XLfit curve fitting program for Microsoft Excel (IDBS, Guildford, Surrey) and expressed as % inhibition of specific [^{3}H]Ro15−1788 binding. From the IC_{50}, K_i was calculated assuming respective K_D values of [^{3}H]Ro15-1788 binding of 0.92, 0.58 and 0.45 nM at the $\alpha1\beta3\gamma2$, $\alpha3\beta3\gamma2$ or $\alpha5\beta3\gamma2$ receptor subtypes.[10]

Functional Efficacy Assays. (a) Voltage Ion Plate Reader (VIPR) Assay for GABA-A α-3 and α-5 Subtypes. Primary functional screening data were generated using a Voltage/Ion Probe Reader assay (VIPR; Aurora Biosciences, CA) largely as previously described.[26,27] Briefly, Ltk$^-$ cells stably expressing $GABA_A$ receptor subunit combinations were seeded into black-sided Porvair 96 well plates, and receptor expression was induced 24 h prior to experiment with 1 μM dexamethasone (Sigma, UK). Cells were washed in low-Cl$^-$ buffer (160 mM sodium D-gluconate, 4.5 mM potassium D-gluconate, 2 mM $CaCl_2$, 1 mM $MgCl_2$, 10 mM D-glucose, 10 mM HEPES pH 7.4) and dye-loaded for 30 min to give final concentrations of 4 μM chlorocoumarin-2-dimyristoyl phosphatidylethanolamine (CC2-DMPE; FRET donor) (Aurora Biosciences Corp, CA) and 1 μM bis(1,3-diethyl-2-thiobarbiturate)-trimethineoxonol ($DiSBAC_2(3)$; FRET acceptor) (Molecular Probes), with 0.5 mM tartrazine (Sigma, UK) present extracellularly. Plate preparation was automated using a CCS-Packard Platetrak. Plates were then placed in a VIPR which performs automated liquid additions and records fluorescence emission from eight wells. A 400DF15 filter was used in the excitation pathway, and 460DF45 and 580DF60 filters were used in the dual emission pathways. Rapid ratiometric FRET measurements were made of GABA-evoked depolarizations as previously described, and the ability of compounds to modulate an EC_{50} response to GABA was examined. Basal fluorescence was read for 8s before addition of test compounds, and a half-maximal concentration of GABA was added 22s later, with fluorescence emissions recorded at 1 Hz.

For each time-point, background fluorescence was subtracted (recorded from wells without cells in the same plate) and the ratio of fluorescence at 460 nm to 580 nm was calculated. GABA-evoked depolarizations were then expressed as a fractional change in this ratio. In house algorithms written as Excel 97 (Microsoft Corp.) macros were used for calculation of fluorescence ratio and GABA responses. All compound plates contained an in-house inverse agonist at the α5 receptor, a benzodiazepine site agonist (alprazolam) and a nonselective benzodiazepine site inverse agonist (DMCM). Test compound efficacy was normalized to that of DMCM on the same plate, which was always taken as −100%. Compound efficacy was measured at these receptors at 300 nM to minimize direct or fluorescence effects of some compounds at higher concentrations and was derived from at least three plates/day screened over a minimum of 2 days.

(b) Whole Cell Patch-Clamp of L(tk$^-$) Cells Stably Transfected with Human GABA-A Receptors. Experiments were performed on L(tk$^-$) cells expressing human cDNA combinations $\alpha1\beta3\gamma2$s, $\alpha3\beta3\gamma2$s and $\alpha5\beta3\gamma2$s. Glass cover-slips containing the cells in a monolayer culture were transferred to a Perspex chamber on the stage of Nikon Diaphot inverted microscope. Cells were continuously perfused with a solution containing 124 mM NaCl, 2 mM KCl, 2 mM $CaCl_2$, 1 mM $MgCl_2$, 1.25 mM KH_2PO_4, 25 mM $NaHCO_3$, 11 mM D-glucose, at pH 7.2, and observed using phase-contrast optics. Patch-pipets were pulled with an approximate tip diameter of 2 μm and a resistance of 4 MΩ with borosilicate glass and filled with 130 mM CsCl, 10 mM HEPES, 10 mM EGTA, 3 mM Mg^+-ATP, pH adjusted to 7.3 with CsOH. Cells were patch-clamped in whole-cell mode using an Axopatch-200B patch-clamp amplifier. Drug solutions were applied by a double-barreled pipet assembly, controlled by a stepping motor attached to a Prior manipulator, enabling rapid equilibration around the cell. Increasing GABA concentrations were applied for 5 s pulses with a 30 s interval between applications. Curves were fitted using a nonlinear square-fitting program to the equation $f(x) = B_{max}/[1 + (EC_{50}/x)^n]$ where x is the drug concentration, EC_{50} is the concentration of drug eliciting a half-maximal response, and n is the Hill coefficient. Allosteric modulation of GABA receptors was measured relative to a GABA EC_{20},

individually determined for each cell to account for differences in GABA affinity.

Stability in Liver Microsomes. Test compound at a concentration of 1 μM in pH 7.4 buffer containing 1% DMSO was incubated at 37 °C for 15 min with liver microsomes (0.5 mg/mL protein concentration) in the presence or absence of NADPH (1 mM). The reaction was quenched by the addition of MeCN and after vortex mixing and centrifugation, samples were analyzed by LC-MS/MS (HP1050/CTC autosampler; KR100 5C18 column, 50 mm × 2.1 mm i.d.; with gradient elution using MeCN in 25 mM ammonium formate pH 3; flow 0.4 mL/min; injection volume 20 μL). A Micromass Quattro LC was used as the mass spectrometer. Turnover was calculated by comparing the peak areas for incubations performed in the presence of NADPH with those performed in the absence of NADPH.

Pharmacokinetic Determinations. The jugular vein of a male Sprague Dawley rat (approximate weight 300 g) was cannulated under isofluorane anaesthesia. The rat was treated with a 100 unit dose of heparin (0.1 mL, 1000 units/mL) via the cannula and then allowed to recover for 48 h. The animal was deprived of food overnight and then given a 1 mg/kg dose of the test compound iv, via bolus injection. The test compound was formulated as a solution (1 mg/mL) in a PEG 300:H_2O (3:1). Serial blood samples (600 μL) were collected into heparinized tubes at several time points up to 6 h after dosing. Plasma was harvested from the blood samples by centrifugation, and the samples were stored at −80 °C until analysis. To 10 μL aliquots of 1 ng/μL internal standard solution (diazepam) on a conical bottomed 96-well plate were added plasma (50 μL) and MeCN (150 μL). The plate was sealed, mixed and centrifuged. A portion of the supernatant (100 μL) was added to 25 mM ammonium formate pH3 (50 μL) on a fresh 96-well plate. The resulting samples were analyzed using the same LC-MS/MS method described above. Detection of test compound was achieved by MRM ESP+ using the transition 258.3 to 77.0. Quantitation of test compound was achieved by comparing peak areas of samples against a calibration curve obtained by spiking control rat plasma with known amounts of test compounds. All pharmacokinetic analysis was model independent and used standard formulas in a Microsoft Excel spreadsheet.

General Chemical Experimental Details. ^{1}H NMR spectra were recorded on Bruker AMX500, AV500, DPX400 or DPX360 spectrometers. Chemical shifts are reported in parts per million (δ) downfield from tetramethylsilane as internal standard and coupling constants in Hertz. Melting points were determined on a Reichert Thermovar hot stage apparatus and are uncorrected. Mass spectra were recorded using a HP1100 flow inject system (50:50 1% formic acid−H_2O:MeCN; 30 s run; flow rate 0.3 mL/min) into an electrospray source of a Waters ZMD2000. Spectra were recorded between 100 and 800 Da. Standard abbreviations are used for common solvents. During workup procedures, organic solvents were dried over $MgSO_4$ prior to concentration. Anhydrous THF, DMF, Et_2O, MeOH, and toluene were purchased from the Aldrich Chemical Co. EtOH refers to absolute EtOH. Flash chromatography and dry flash chromatography were performed on silica gel Merck Kieselgel (230−400) mesh and Merck 15111, respectively. Thin-layer chromatography (TLC) was carried out on Merck 5 × 10 cm plates with silica gel 60 F254 as sorbant. Preparative thin-layer chromatography was carried out using 20 × 20 cm silica gel GF tapered plates supplied by Analtech Inc, Newark. Phase separation cartridges were supplied by Whatman (12 mL volume with 5 μM pore size PTFE membrane). Mass triggered preparative LC-MS was run on a Waters Fraction Lynx running 10 min gradients (20 mL/min, 0.1% TFA−H_2O/MeCN) through a Supelco ABZ+ column. Microanalysis was determined by Butterworth Laboratories, 54−56 Waldegrave Road, Teddington, U.K. Microwave reactions were carried out, unless indicated, using a Smith Synthesizer supplied by Personal Chemistry, Uppsala, Sweden. Details of HPLC conditions used to analyze target compounds is provided in the Supporting Information section. Purity for target compounds was ≥95% as judged by NMR and HPLC. Representative procedures for the synthesis of compounds **15**, **23**, **29**, and **36** are given below. Alternative procedures to 5-(3-bromophenyl)−(*2H*)-pyridazin-3-one (**11**, Ar = 3-Br-Ph), 5-(3-bromophenyl)-3-chloropyridazine (**12**, Ar = 3-Br-Ph) and 3-(6-ethylaminopyridazin-4-yl)-benzonitrile (**38**) is available in Supporting Information. 2,4-Diphenylpyridine, 3,5-diphenylpyridine, 4,6-diphenylpyrimidine and 3,5-diphenyl-1,2,4-triazine are commercially available. 4,6-Diphenyl-1,2,3-triazine was prepared using literature procedures.[28]

Representative Stille and Suzuki Couplings for Synthesis of 3-Phenyl-5-arylpyridazines (13−22). 3-(6-Phenylpyridazin-4-yl)benzonitrile (15). (a) 5-(Tri-*n*-butylstannyl)-3-phenyl pyridazine[20] (**8**) (100 mg, 0.22 mmol), 3-bromobenzonitrile (48 mg, 0.27 mmol) and palladium(0) tetrakis-(triphenylphosphine) (5 mg) in 4 mL of THF were combined and heated to 150 °C for 600 s in microwave reactor. The reaction was diluted with 6 mL of CH_2Cl_2 and 2 mL of H_2O then poured into a phase separation cartridge. The organic phase was collected and concentrated to leave ∼100 mg of crude product. Part of the sample was purified by HPLC with mass triggered fraction collection to give (**15**) (2.2 mg). Purification could also be carried out by preparative thin-layer chromatography using 1:1 EtOAc−hexanes as eluent or recrystallization from MeOH or ^{i}PrOH.

(b) 5-Iodo-3-phenylpyridazine[20] (**9**) (480 mg, 1.17 mmol), 3-cyanophenylboronic acid (200 mg, 1.17 mmol), and palladium(0) tetrakis(triphenylphosphine) (40 mg) in 4 mL of THF and 0.5 mL of 2 N Na_2CO_3 were reacted and purified as described above to give (**15**) (84 mg, 28%). δ_H (400 MHz, DMSO-d_6) 7.57−7.64 (3H, m), 7.81 (1H, t, J = 8 Hz), 8.03 (1H, d, J = 8 Hz), 8.30−8.35 (2H, m), 8.41 (1H, d, J = 8 Hz), 8.59 (1H, d, J = 4 Hz), 8.63 (1H, s), 9.69 (1H, d, J = 4 Hz). *m/z* (ES+) 258 (MH^+). Mp. 170−171 °C. Anal. ($C_{17}H_{11}N_3$) C, H, N.

Representative Synthesis of 3,5-Diarylpyridazines (23−27, 41). 3-[6-(2-Fluorophenyl)-pyridazin-4-yl]benzonitrile (23). (a) 5-Chloropyridazin-3(2*H*)-one (**10**) (2.0 g, 15.3 mmol), dichloro-(1,4-bis(diphenylphosphino)butane) (0.1 g, 0.16 mmol), 3-cyanophenylboronic acid (2.71 g, 18.4 mmol) and saturated Na_2CO_3 solution (5 mL) in 20 mL of toluene were combined and heated to 120 °C for 15 min in a Milestone microwave reactor. The reaction was filtered and the solid washed with ^{i}PrOH (20 mL) then dried to give 5-(3-cyanophenyl)pyridazine-3-one (**11**, Ar = 3-CN-Ph) as a yellow solid (1.8 g, 50%). δ_H (400 MHz, DMSO-d_6) 7.20 (1H, m), 7.79 (1H, t, J = 8 Hz), 8.05 (1H, m), 8.33 (1H, m), 8.54 (1H, m), 8.37 (1H, m), 13.1 (1H, br s). *m/z* (ES+)197 (MH^+).

(b) 5-(3-Cyanophenyl)pyridazin-3-one (**11**, Ar = 3-CN-Ph) (1.8 g, 9.1 mmol) was suspended in phosphorus oxychloride (15 mL, 12 mmol) and heated to 100 °C for 1 h. The reaction was cooled to room temperature and concentrated under reduced pressure before being poured onto ice. The pH was adjusted to 8 by portionwise addition of saturated Na_2CO_3 solution, and the resultant solid was collected by filtration, washed with H_2O, and dried to give 3-chloro-5-(3-cyanophenyl)-pyridazine (**12**, Ar = 3-CN-Ph) (1.5 g, 76%). δ_H (400 MHz, DMSO-d_6) 7.79 (1H, t, J = 8 Hz), 8.05 (1H, m), 8.33 (1H, m), 8.41 (1H, d, J = 2 Hz), 8.54 (1H, m), 9.75 (1H, m). *m/z* (ES^+) 216, 218 (MH^+).

(c) 3-Chloro-5-(3-cyanophenyl)pyridazine (**12**, Ar = 3-CN-Ph) (0.1 g, 0.46 mmol), 2-fluorophenyl boronic acid (80 mg, 0.572 mmol), palladium(0) tetrakis(triphenylphosphine) (25 mg) and saturated Na_2CO_3 solution (0.5 mL) in 1.5 mL of THF were combined and heated to 150 °C for 600 s in a microwave reactor. The reaction was diluted with 6 mL of CH_2Cl_2 and 2 mL of saturated NH_4Cl then poured into a phase separation cartridge. The organic phase was concentrated and purified by column chromatography using 30 to 40% EtOAc/hexanes as eluent to give (**23**) as a colorless solid (65 mg, 51%). δ_H (400 MHz, DMSO-d_6) 7.43−7.48 (2 H, m), 7.60−7.66 (1 H, m), 7.80 (1 H, t, J = 7.8 Hz), 7.98−8.02 (1 H, m), 8.02−8.04 (1 H, m), 8.34−8.37 (1 H, m), 8.42 (1H, t, J = 2.0 Hz), 8.56−8.57 (1 H, m), 9.75 (1 H, d, J = 2.0 Hz). *m/z* (ES+) 276 (MH^+).

Representative Synthesis of 3-Alkoxy-5-arylpyridazines (28−31). 5-(3-Bromophenyl)-3-ethoxy pyridazine (29). (a) Sodium metal (0.13 g, 5.65 mmol) was added portionwise to dry ethanol (10 mL) using external H_2O bath cooling. On addition of all the sodium, the reaction was allowed to attain room temperature and the solution stirred for 1 h before adding 5-(3-bromophenyl)-3-chloropyridazine (**12**, Ar = 3-Br-Ph) (0.15 g, 0.557 mmol) in EtOH (5 mL). The suspension was stirred for 18 h before adding H_2O and removing the EtOH in vacuo. The products were extracted into CH_2Cl_2, concentrated, and purified by preparative TLC using 25% EtOAc/hexanes as eluent to give (**29**) as a colorless solid (30 mg, 19%). δ_H (400 MHz, DMSO-d_6) 1.41 (3 H, t, J = 7.0 Hz), 4.55 (2 H, q, J = 7.0 Hz), 7.50 (1 H, t, J = 8.0 Hz), 7.55 (1 H, d, J = 2.0 Hz), 7.71−7.74 (1 H, m), 7.91−7.94 (1 H, m), 8.14 (1 H, t, J = 1.8 Hz), 9.30 (1 H, d, J = 2.0 Hz). 1H. *m/z* (ES^+) 279, 281 (MH^+).

Representative Synthesis of 3-Alkylamino-5-arylpyridazines (34−40). [5-(3-Bromophenyl)-*N*-pyridazin-3-yl]ethylamine (36). To 5-(3-bromophenyl)-3-chloropyridazine (**12**, Ar = 3-Br-Ph) (1.2 g, 4.46 mmol) was added to a 2 M solution of ethylamine in THF (7 mL) and heated to 170 °C for 1 h in a microwave reactor. The organic phase was diluted with EtOAc, washed with H_2O, dried and concentrated while loading onto silica. Column chromatography using a gradient of 20% EtOAc/hexanes to EtOAc as eluent gave (**36**) as an orange solid (0.45 g, 36%). δ_H (360 MHz, DMSO-d_6) 1.20 (3 H, t, J = 7.0 Hz), 3.41 (2 H, qd, J = 5.5, 7.0 Hz), 6.84 (1 H, t, J = 5.5 Hz), 6.99 (1 H, d, J = 2.0 Hz), 7.49 (1 H, t, 7.8 Hz), 7.68−7.71 (1 H, m), 7.74−7.77 (1 H, m), 7.95 (1 H, t, J = 1.8 Hz), 8.79 (1 H, d, J = 2.0 Hz). *m/z* (ES^+) 278, 280 (MH^+).

Acknowledgment. We thank Philip Jones, Matthew Lindon, Elizabeth Norris, Jonathan Rose and Paul Scott-Stevens for their contributions to this work.

Supporting Information Available: NMR and mass spectral data for compounds **13**, **14**, **16-22**, **24−28**, **30−35**, **37**, **39−41**, microanalysis data for **15** and HPLC data for **13**, **14**, **16−41**. Alternative procedures to 5-(3-bromophenyl)-(2*H*)-pyridazin-3-one (**11**, Ar = 3-Br-Ph), 5-(3-bromophenyl)-3-chloropyridazine (**12**, Ar = 3-Br-Ph) and 3-(6-ethylaminopyridazin-4-yl)benzonitrile (**38**). This material is available free of charge via the Internet at http://pubs.acs.org.

References

(1) McNamara, R. K.; Skelton, R. W. The neuropharmacological and neurochemical basis of place learning in the Morris water maze. *Brain Res. Rev.* **1993**, *18*, 33−49. DeLorey, T. M.; Lin, R. C.; McBrady, B.; He, X.; Cook, J. M.; Lameh, J.; Loew, G. H. Influence of benzodiazepine binding site ligands on fear-conditioned contextual memory. *Eur. J. Pharmacol*, **2001**, *426* (1, 2), 45−54. Bailey, D. J.; Tetzlaff, J. E.; Cook, J. M.; He, X.; Helmstetter, F. J. Effects of hippocampal injections of a novel ligand selective for the α5β2γ2 subunits of the GABA/benzodiazepine receptor on Pavlovian conditioning. *Neurobiol. Learn. Mem*. **2002**, *78* (1), 1−10. Liu, R.; Hu, R. J.; Zhang, P.; Skolnick, P.; Cook, J. M. Synthesis and pharmacological properties of novel 8-substituted imidazobenzodiazepines: high-affinity, selective probes for alpha 5-containing GABAA receptors. *J. Med. Chem.* **1996**, *39* (9), 1928−34.

(2) Whiting, P. J. The GABA-A receptor gene family: new targets for therapeutic intervention. *Neurochem. Int.* **1999**, *34* (5), 387−390.

(3) Pritchett, D. B.; Sontheimer, H.; Shivers, B. D.; Ymer, S.; Kettenmann, H.; Schofield, P. R.; Seeburg, P. H. Importance of a novel GABAA receptor subunit for benzodiazepine pharmacology. *Nature* **1989**, *338*, 582−585.

(4) Wisden, W.; Laurie, D. J.; Monyer, H.; Seeburg, P. H. The distribution of 13 GABAA receptor subunit mRNA's in the rat brain. *J. Neurosci.* **1992**, *12*, 1040−1062.

(5) Collinson, N.; Kuenzi, F. M.; Jarolimek, W.; Maubach, K. A.; Cothliff, R.; Sur, C.; Smith, A.; Otu, F. M.; Howell, O.; Atack, J. R.; McKernan, R. M.; Seabrook, G. R.; Dawson, G. R.; Whiting, P. J.; Rosahl, T. W. Enhanced learning and memory and altered GABAergic synaptic transmission in mice lacking the α5 subunit of the GABAA receptor. *J. Neurosci.* **2002**, *22* (13), 5572−5580.

(6) Crestani, F.; Keist, R.; Fritschy, J.-M.; Benke, D.; Vogt, K.; Prut, L.; Bluthmann, H.; Mohler, H.; Rudolph, U. Trace fear conditioning involves hippocampal α5 GABAA receptors. *Proc. Natl. Acad. Sci. U.S.A.* **2002**, *99* (13), 8980−8985.

(7) Whiting, P. J. GABA-A receptor subtypes in the brain: a paradigm for CNS drug discovery? *Drug Discovery Today* **2003**, *8* (10), 445−450.

(8) Whiting, P. J.; Wafford, K. A.; McKernan, R. M. Pharmacologic subtypes of GABAA receptors based on subunit composition. *GABA Nerv. Sys.* **2000**, *113* (126), 113−116.

(9) Quirk, K.; Gillard, N. P.; Ragan, C. I.; Whiting, P. J.; McKernan, R. M. Model of subunit composition of gamma-aminobutyric acid A receptor subtypes expressed in rat cerebellum with respect to their alpha and gamma/delta subunits. *J. Biol. Chem*. **1994**, *269*, 16020−16028.

(10) Hadingham, K. L.; Wingrove, P.; Le Bourdelles, B.; Palmer, K. J.; Ragan, C. I.; Whiting, P. J. Cloning of cDNA sequences encoding human α-2 and α3 γ-aminobutyric acid A receptor subtypes and characterisation of the benzodiazepine pharmacology of recombinant of α1-, α2-, α3 and α5-containing human γ-aminobutyric acid A receptors. *Mol. Pharmacol*. **1993**, *43*, 970−2975.

(11) Cooke, A. J.; Hamilton, N. M. *Expert Opin. Ther. Pat.* **2002**, *12* (10), 1491−1501.

(12) Chambers, M. S.; Atack, J. R.; Broughton, H. B.; Collinson, N.; Cook, S.; Dawson, G. R.; Hobbs, S. C.; Marshall, G.; Maubach, K. A.; Pillai, G. V.; Reeve, A. J.; MacLeod, A. M. Identification of a novel, selective GABAA α5 receptor inverse agonist which enhances cognition. *J. Med. Chem*. **2003**, *46* (11), 2227−2240.

(13) Sternfeld, F.; Carling, R. W.; Jelley, R. A.; Ladduwahetty, T.; Merchant, K. J.; Moore, K. W.; Reeve, A. J.; Street, L. J.; O'Connor, D.; Sohal, B.; Atack, J. R.; Cook, S.; Seabrook, G.; Wafford, K.; Tattersall, F. D.; Collinson, N.; Dawson, G. R.; Castro, J. L.; MacLeod, A. M. Selective, orally active γ-aminobutyric acid-A α5 receptor inverse agonists as cognition enhancers. *J. Med. Chem*. **2004**, *47* (9), 2176−2179.

(14) Street, L. J.; Sternfeld, F.; Jelley, R. A.; Reeve, A. J.; Carling, R. W.; Moore, K. W.; McKernan, R. M.; Sohal, B.; Cook, S.; Pike, A.; Dawson, G. R.; Bromidge, F. A.; Wafford, K. A.; Seabrook, G. R.; Thompson, S. A.; Marshall, G.; Pillai, G. V.; Castro, J. L.; Atack, J. R.; MacLeod, A. M. Synthesis and biological evaluation of 3-heterocyclyl-7,8,9,10-tetrahydro-(7,10-ethano)-1,2,4-triazolo-[3,4-a]phthalazines and analogues as subtype-selective inverse agonists for the GABAAα5 benzodiazepine binding site. *J. Med. Chem*. **2004**, *47* (14), 3642−3657.

(15) Chambers, M. S.; Atack, J. R.; Carling, R. W.; Collinson, N.; Cook, S. M.; Dawson, G. R.; Ferris, P.; Hobbs, S. C.; O'Connor, D.; Marshall, G.; Rycroft, W.; MacLeod, A. M. An orally bioavailable, functionally selective inverse agonist at the benzodiazepine site of $GABA_A$ α5 receptors with cognition enhancing properties. *J. Med. Chem*. **2004**, *47* (24), 5829−5832.

(16) Komendantov, M. I.; Bekmukhametov, R. R. 1,3-Dipolar cycloaddition of diazomethane to the cyclopropene double bond, and new method for synthesizing bicyclobutane derivatives. *Zh. Org. Khim.* **1971**, *7* (2), 423−424.

(17) Huber, M. K.; Martin, R.; Rey, M.; Dreiding, A. S. The aminal-enamine equilibrium in cyclopropane carbaminals. *Helv. Chim. Acta* **1977**, *60* (5), 1781−1800.

(18) Komendantov, M. I.; Bekmukhametov, R. R.; Novinskii, V. G. 1,3-Dipolar cycloaddition of diazomethane to the cyclopropene double bond. New method for the synthesis of bicyclobutane derivatives. *Zh. Org. Khim.* **1976**, *12* (4), 801−805.

(19) Goodnow, R. Small molecule lead generation processes for drug discovery. *Drugs Future* **2002**, *27* (12), 1165−1180.

(20) Sauer, J.; Heldman, D. K. Synthesis of 3,5−disubstituted pyridazines by regioselective [4+2] cycloadditions with ethynyltributyltin and subsequent replacement of the organotin substituent. *Tetrahedron* **1998**, 54 (17), 4297−4312.

(21) Oprea, T. I.; Davis, A. M.; Teague, S. J.; Leeson, P. D. Is There a difference between leads and drugs? A historical perspective. *J. Chem. Inf. Comput. Sci.* **2001**, *41*, 1308−1315.

(22) Hann, M. M.; Leach, A. R.; Harper, G. Molecular complexity and its impact on the probability of finding leads for drug discovery. *J. Chem. Inf. Comput. Sci*. **2001**, *41*, 856−864.

(23) The use of microwaves in synthesis is gaining momentum with the introduction of sophisticated reactors that enable multiple reactions to be run safely, with short reaction times: Lidstrom, P.; Tierney, J.; Wathey, B.; Westman, J. Microwave assisted organic synthesis- a review. *Tetrahedron* **2001**, *57*, 9225−9283.

(24) The selection of the commercially available aryl halides was made by searching the Available Chemicals Directory (ACD) for all mono-bromo or chloro substituted phenyl derivatives that did not contain additional reactive functional groups. The list was further reduced by considering only preferred suppliers and using a molecular weight <300. This set of structures was then

clustered into 10 clusters using k-means clustering on topological similarities calculated from our in-house 2D descriptors: Kearsley, S. K.; Sallamack, S.; Fluder, E. M.; Andose, J. D.; Mosley, R. T.; Sheridan, R. P. *J. Chem. Inf. Comput. Sci*. **1996**, *36*, 118. Any cluster with more than five-members was itself clustered and so forth in a recursive fashion. A set of 50 aryl bromides was then selected from across the clusters and the similarity matrix of the final selection was inspected to confirm that a diverse set of reagents had been chosen. This set was used in the first parallel run and subsequent iterative parallel runs used other members of the reagent sets when the first reagent used was demonstrated to lead to high affinity pyridazines.

(25) Francisco, F. P.; Celia, E. G. 3(2H)-Pyridazinones. ES 454136, 1977.

(26) Adkins, C. E.; Pillai, G. V.; Kerby, J.; Bonnert, T. P.; Haldon, C.; McKernan, R. M.; Gonzalez, J.; Oades, K.; Whiting, P. J.; Simpson, P. B. $\alpha_4\beta_3\delta$ GABA$_A$ receptors characterized by fluorescence resonance energy transfer-derived measurements of membrane potential. *J. Biol. Chem*. **2001**, *276*, 38934−38939.

(27) Smith A. L.; Oxley, B.; Malpas, S.; Pillai, G. V.; Simpson, P. B. Compounds exhibiting selective efficacy for different β subunits of human recombinant GABAA receptors. *J. Pharmacol. Exp. Ther*. **2004**, *311*, 601−609.

(28) Ohsawa, A.; Arai, H.; Ohnishi, H.; Itoh, T.; Kaihoh, T.; Okada, M.; Igeta, H. Oxidation of 1-aminopyrazoles and synthesis of 1,2,3-triazines. *J. Org. Chem*. **1985**, *50* (26), 5520−5523.

JM050249X